Journal of Applied Fluid Mechanics, Vol. 9, No. 2, pp. 625-633, 2016.
Available online at www.jafmonline.net, ISSN 1735-3572, EISSN 1735-3645.
DOI: 10.18869/acadpub.jafm.68.225.24446

Obstacle Geometry Effect on the Stability of Two-Dimensional Incompressible Flow in a Channel

S. Fezai†, N. Ben-Cheikh, B. Ben-Beya and T. Lili

University of Tunis El Manar, Faculty of Sciences of Tunis, Laboratory of fluid Mechanics, physics department, 2092, Tunis, Tunisia.

†*Corresponding Author Email:fezai.salwa@gmail.com*

(Received January 2, 2015; accepted March 28, 2015)

ABSTRACT

Two-dimensional incompressible fluid flow around a rectangular shape placed over a larger rectangular shape is analyzed numerically. The vortex shedding is investigated at different arrangements of the two shapes. The calculations are carried out for several values of Reynolds numbers from low values up to 52. At low Reynolds number, the flow remains steady. The flow characteristics are analyzed for each configuration. The analysis of the flow evolution shows that with increasing Re beyond a certain critical value, the flow becomes unstable and undergoes a bifurcation. It is observed that the transition to unsteady regime is performed by a Hopf bifurcation. The critical Reynolds number beyond which the flow becomes unsteady is determined for each configuration.

Keywords: Obstacle; Incompressible fluid flow; Finite-volume method; Von Karman vortex street; Critical Reynolds number.

NOMENCLATURE

Re	channel Reynolds number	St	Strouhal number
CD	drag coefficient	(u, v)	velocity components, m s^{-1}
CL	lift coefficient	ν	viscosity, m^2s^{-1}
c	critical	(x,y)	dimensionless coordinates
h	channel height		
l	channel width	ϕ	generic variable
p	dimensionless pressure	ρ	density of fluid, kg m^{-3}
Max,Min	maximum, minimum		

1. INTRODUCTION

Flows around objects are phenomena that occur frequently in practice. Their understanding is essential in the mechanical and thermal design of many engineering systems such as: airplanes, automobiles, buildings, electronic components, turbine blades and geometric shapes of square and circular section. The identification and study of hydro and aerodynamic phenomena that arise in the wake of an obstacle remains a topic of current interest in various fields. Besides, wake around obstacles is a major interest in practice. Indeed, the knowledge structures generated behind these barriers and their plans is of paramount in the design of fluid flows exposed to utility works. The choice of the study of cylindrical and square obstacles is resulting from their simple geometry that facilitates experimental and numerical investigations (Bhattacharyya and Dhinakaran (2008), Straatman and Martinuzzi (2003), Guo and Julien (2008), Wang *et al*. (2014)). Many researches works have been made to model the flow around obstacles. In this vein, several experiments in the field were performed and compared to numerical methods. In this context, a wide range of mathematical methods have been developed to approach the reality of flow and provide maximum results that may occur. Breuer *et al*. (2000) studied numerically the flow around a square cylinder inside a channel by both numerical methods: a Lattice-Boltzmann and finite volume method. They made a comparison between the results of these two methods and found that when Re <60, there is an excellent agreement between the two methods for the computation of the length of the recirculation zone, but they detected a small difference to the

drag coefficient. When Re increases to 100, they measured the velocity profiles at different locations and found a good agreement. At Re =150, the two methods give a local maximum of the Strouhal number and the authors concluded that the differences between both numerical techniques are almost negligible.

Berrone *et al*. (2011) made a comparison between the two finite volume methods and finite elements. They studied a flow around a cylinder with two different ratios of blocking one B/D=5 (rectangular cylinder) and the other B/D=1 (square cylinder). They found good agreement between the results of two techniques for both cylinders and for different flow regimes.

These researchers have also shown the influence of Reynolds number on the criteria of occurrence of different regimes such as crawling system, the steady regime and unsteady.

In addition, the steady flow around a circular cylinder in a channel with a moving wall for a Reynolds number ranging from 50 to 200 has been investigated by Qu *et al*. (2013). The authors recorded a non-monotonous stream-wise velocity recovery in the intermediate wake for Re>50, a phenomenon that has been grossly overlooked in the past. Furthermore, the variation of field was seen to have no effect on the size of the vortices behind the obstacle and also the angles of separation.

On another hand, many authors also analyzed the effect of the time parameter on the flow regime but they found that this parameter has little influence on the drag coefficient on and the Strouhal number.

Zhou *et al*. (2005) carried out a numerical study on the reduction of fluid forces acting a square cylinder in a two-dimensional channel using a control plate. The forces acting on the cylinder, the frequency of vortex formation and the various schemes are designed for different heights and positions of the control plate. They also found that the existence of the plate changes the characteristics of the upstream flow of the cylinder completely. Subsequently, they determined the optimal position of the control plate for each height in order to minimize the drag force effects along the cylinder.

Another numerical analysis focusing on the effect of the geometry of the barrier has been performed by Franke *et al*. (1990). They noted that the flow around a square cylinder behaves similarly to the case of the flow around a circular cylinder, the main difference was in the fact that the separation points are fixed to the sharp corners of the cylinder. They investigated the effect of Reynolds number on the Strouhal value by processing the corner regions which may affect the vortex-shedding frequency due to high velocity gradients in these corners. Thereafter, they discussed the structure of the flow for both obstacles and they concluded that the variation of the lift and drag forces for low Reynolds is similar for both obstacles but the difference appears for large Reynolds.

Furthermore, Mukhopadhay *et al*. (1992) analyzed the structure of a flow around a square obstacle for different Reynolds numbers and different positions of the obstacle. These authors were able to determine the vortex-shedding frequency using the spectral analysis of the temporal evolution of the coefficient. Consequently, they determined the critical Reynolds number from which the flow becomes periodic and they concluded that the frequency starts at Re = 87 for a blockage ratio B / H = 0.25.

The transition from a symmetric flow state to the periodic state was also well analyzed by Turki *et al*. (2003). They found the critical value of Re which was observed to increase with the blockage ratio. In addition, the Reynolds numbers corresponding to the maximum of the Strouhal number and the minimum of the time averaged drag coefficient were seen to strongly depend on this parameter and were observed at Re =130, 140 and 150 for the blocking ratio values 1/8, 1/6 and 1/4, respectively. The authors also declared that for a high blockage ratio and Re numbers, the square cylinder has a stable transversal posture to the flow.

Bhattacharyya and Maiti (2004) numerically analyzed the structure of the wake behind a square cylinder placed near the lower wall. They found that the wall causes a difference in strength between the two rows of vortices and it was found that the strength of the positive vortices from the lower portion of the cylinder decreases with the decrease in the barrier height between the bottom wall and the obstacle.

The aim of the present paper is to analyze the effect of changing the geometry of the obstacle on the flow structure and to determine the critical Reynolds number for each configuration of the obstacle from which the flow exhibits an unsteady behavior.

2. PHYSICAL PROBLEM

The configuration of this problem consists of a two dimensional flow of a Newtonian incompressible fluid around an obstacle situated in a channel having a width l = 50H and a height h = 8H as sketched in Figure 1.

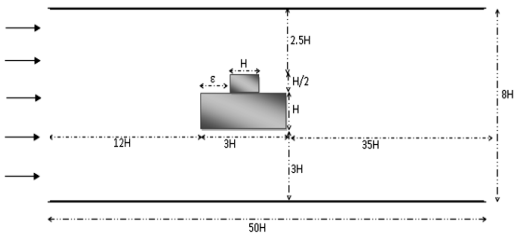

Fig. 1. Physical model.

In the present study, three configurations will be considered by varying the value of ε between 0 and 2H.

For the configuration (1), the value of ε is set to

H,the value of ε for the second configuration is 0, while the value of ε relative to the third configuration is kept at

ε = 2H.

2.1 Governing flow Equations

The flow is assumed to be two-dimensional of an incompressible Newtonian fluid, around an obstacle that is governed by the dimensionless Navier-Stokes equations, which describes the continuity and momentum equations in Cartesian coordinates (i, j= 1, 2) written as:

$$\frac{\partial u_i}{\partial x_i} = 0 \tag{1}$$

$$\frac{\partial u_i}{\partial t} + \frac{\partial (u_i u_j)}{\partial x_j} = -\frac{\partial p}{\partial x_i} + \frac{1}{\mathrm{Re}} \frac{\partial^2 u_i}{\partial x_j \partial x_j} \tag{2}$$

Generally, a dimensionless writing of the Navier-Stokes equations shows the usual dimensionless numbers. These parameters characterize the similarity structure and stability of the flow. It is worth noting that the scales H, u_e, $p_0 = (1/2)\rho_0 u_e^2$ and $t_0 = (H / u_e)$ are used for the dimensionalization of the coordinate space x_i=(x,y), velocity u_i=(u,v), pressure p and time t respectively.

In the momentum equation, a dimensionless number appears that is the Reynolds number expressed by:

$$\mathrm{Re} = (u_e H / \nu)$$

Where u_e is the velocity upstream, H is the side of the barrier and ν is the kinematic viscosity of the fluid under consideration. This dimensionless number characterizes the relationship between inertial forces and viscous ones and thus inertia forces are destabilizing when viscous forces are stabilizing.

2.2 Boundary Conditions

The boundary conditions for this physical problem are as following:

At the channel entrance:

The horizontal u- velocity component has a uniform form u = 1

The vertical component of the velocity v is set to zero.

On the obstacle, non slip conditions are imposed; u = 0 and v = 0

At the exit of the channel:

We use a boundary condition of convective type as this condition appears to be more effective in reducing the computation time and has a slight influence on the velocity. However, the governing parameters such as the Strouhal number and the drag and lift coefficients are roughly assigned by this condition (Sohankar *et al*. 1998).

Convective condition is written as follows:

$$(\partial u_i / \partial t) + u_{conv}(\partial u_i / \partial x) = 0$$

Where $u_{conv} = u_e = 1$

At the upper and lower walls:

The adherence condition (no-slip on the walls) is used.

$(\partial u / \partial x) = 0$ and v= 0

3. NUMERICAL METHOD

The equations governing the flow are nonlinear and have no analytical solution, where the need to use a numerical method.

In our study the resolution of the Navier-Stokes equations is made using the finite volume method (Hortmann *et al*. 1990). This method is used to discretize the equations and the projection method (Brown *et al*. 2001) is also implemented to couple the momentum and continuity equations. Solving these equations was performed using an iterative method RBSOR (Red-Black Successive Over Relaxation) (Ben Cheikh *et al*. 2007). The Poisson pressure correction equation is solved using a full multigrid method as suggested by Ben-Cheikh *et al*. (2008).

The construction of the mesh is the first step in any numerical simulation. This construction consists not only on the number of grid points but also their size and shape. The meshes we have used are based on a staggered grid where scalar quantities (pressure ...) are located at the center of the cell while the velocity components are defined at the centers of faces of the volume controls.

For enhanced accuracy, the grids have denser clustering at the vicinity of the barrier where strong gradients are expected. Conversely, away from the obstacle where the expected gradients are low, larger meshes are preferred.

The convergence of the numerical results is established at each time step according to the following criterion: $\sum \left| \phi_{i,j}^{l} - \phi_{i,j}^{l-1} \right| < 10^{-6}$

The generic variable ϕ stands for u, v or ϕ and l indicates the iteration time levels. In the above inequality, the subscript sequence (i, j) represents the space coordinates x and y.

4. RESULTS AND DISCUSSIONS

4.1 Code Validation

To give more confidence to the results of our numerical simulations, we established some quantitative and qualitative comparisons with other numerical investigations presented in the literature.

Numerical simulations are related to the problem of a square obstacle in a channel where horizontal dimensionless velocity component at the entrance

has a parabolic shape $u_e = (4/64) \times y(8-y)$ and the vertical component is set to zero. The dimensions of the channel and the obstacle are those of physical model of Breuer *et al.* (2000).

The simulations were performed on a non-uniform mesh size m×n=768×160. Breuer *et al.* (2000) used three different grids 500×80, 400×240 and a 560×340. This last mesh was chosen to validate our results with the corresponding ones.

We conducted our study over a range of Reynolds which varies from 60 to 200 and analyzed the effect of this parameter on the evolution of the Strouhal number.

We start with studying the effect of Re on the Strouhal number (Figure 2). It is noted that for relatively low Reynolds numbers (50 < Re < 130) the Strouhal number increases with Re values. A significant change in the structure of flow takes place, namely the movement of separation point of the trailing edge to the leading edge of the square cylinder. The Strouhal number is at a maximum at nearly Re = 140 then decreases again for higher Reynolds numbers.

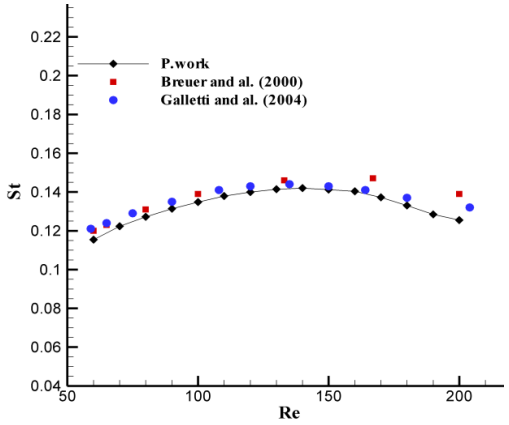

Fig. 2. Variation of the Strouhal values versus the Reynolds number.

Figure 2 shows that our results are in good agreement with the results of Breuer *et al.* (2000) and Galleti *et al.* (2004).As observed, this comparison validates our computer code making confidence on the presented results.

4.2 Effect of Reynolds Number on the flow Patterns

In this sub-section we attempt to reveal the influence of the Reynolds number on the flow patterns. Figure 5 depicts the effect of Reynolds number on the iso-vorticities for the three considered configurations considered. For Re <Rec the flow is stable and steady, and the flow structure is symmetrical with respect to the longitudinal axis. Downstream of the obstacle, a wake appears formed by two nearly symmetric counter rotating vortices attached to the obstacle.

As the Reynolds number is increased above Rec, a change in vortex is observed with a development of the vortex street of Von- Karman and an increase in the wake zone. It is worth noting that this phenomenon is due to a repeating pattern of swirling vortices caused by the unsteady separation of flow of a fluid around blunt the body. In fact, we may observe the emergence of alternate pair of vortices of opposite signs that stands behind the cylinder. By further increasing the Reynolds number, flow instabilities are enhanced and the flow undergoes an oscillatory trend. Thus, the fluctuation in the wake is purely periodic showing an increase in the amplitude and a variable frequency in the laminar regime. We also note the formation of large vortices that develop and are sometimes ejected alternately to the top wall and the bottom wall. One can deduce that there are rolling eddies in the wake zone with a non-slip situation (Figure 3).

4.3 Critical Reynolds Number for the three Configurations

Stability analysis, local or global, has taken more attention in fluid mechanics researches in recent years in order to understand the flow transition from one regime to another. Indeed the transition between the recirculation bubble and driveway Periodical Von-Karman vortex is widely studied in the literature.

For better understanding of the phenomenon, one can refer to the investigation of Yang and Zebib(1989). They showed that when the Reynolds number of about 20, an absolutely unstable region begins to form, and grows more and more with Re. Furthermore, they deduced that the critical Reynolds number corresponds to a state where all wake is absolutely unstable.

Noack and Eckelmann (1994) have analyzed the effect of Reynolds number on the different instabilities that may occur in the wake of a cylinder using the Galarkin method. Furthermore, they found that for all Reynolds less than 54 the flow is stable, while the periodicity appears for 54 <Re <170.Two solutions of supercritical Hopf bifurcation for Re = 54 and Re = 170 were predicted from which the flow passes to a periodic three-dimensional appearance established.

Kelkar and Patankar (1992) have focused on the study of instability that causes a steady laminar flow behind a square cylinder to result in an unstable laminar flow.

Indeed, they showed that the point of instability is between Re = 50 and 60 and they computed the value of the critical Reynolds number having a value Rec=53.

At this stage, we can conclude that the flow is oscillatory from a certain value of Reynolds. This periodic behavior occurs when the Reynolds number exceeds the critical value of Reynolds from which the flow becomes unsteady.

Indeed, we performed multiple calculations for Reynolds number for the three configurations.

We conduct our simulations so we find that the oscillatory flow regime remains beyond Rec and a

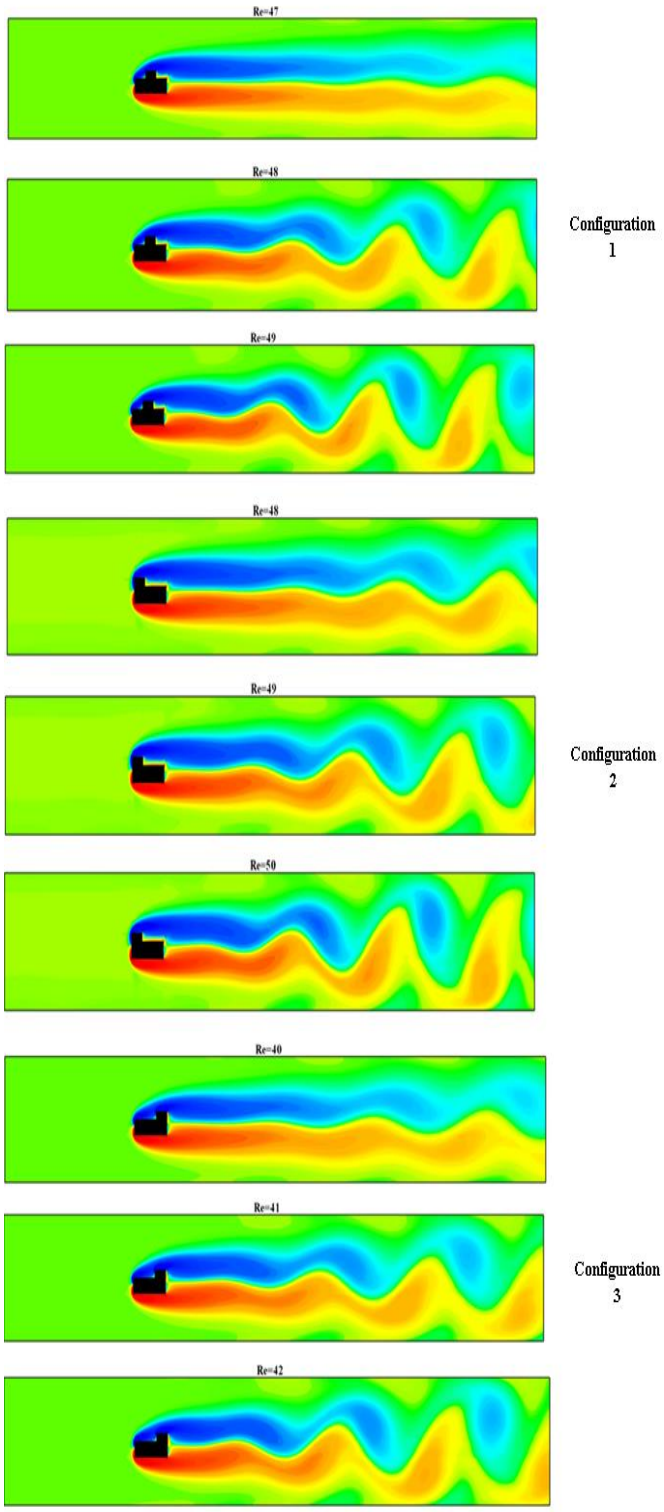

Fig. 3. Flow patterns for the three configurations investigated.

regular flow cannot persist beyond this Reynolds number.

In addition, we find that the amplitude of the oscillations increases with Re. This dependence is illustrated for the three configurations in Figure 4 relatively to the u-velocity component at location (x=18; y=4.4) for the three considered configurations. It can be seen that all the velocity components are oscillates with sinusoidal periodic signal.

To check the periodic behavior of the flow, a phase diagram of the vertical v-velocity component depending on the longitudinal u-velocity component for different Re values is shown in Figure 5.

In addition, as seen in Figure 3, the flow exhibits an oscillatory trend after the critical point. It becomes unstable and periodic in time and the bifurcation point instability is a Hopf bifurcation (Chen *et al.* (1995), Sahin and Owens (2004), Jackson (1987)). The square root of the amplitude of the solution increases with the bifurcation parameter. This means that the square of the amplitude of the longitudinal and vertical u- and v-velocity components must be proportional to the Re value after the bifurcation.

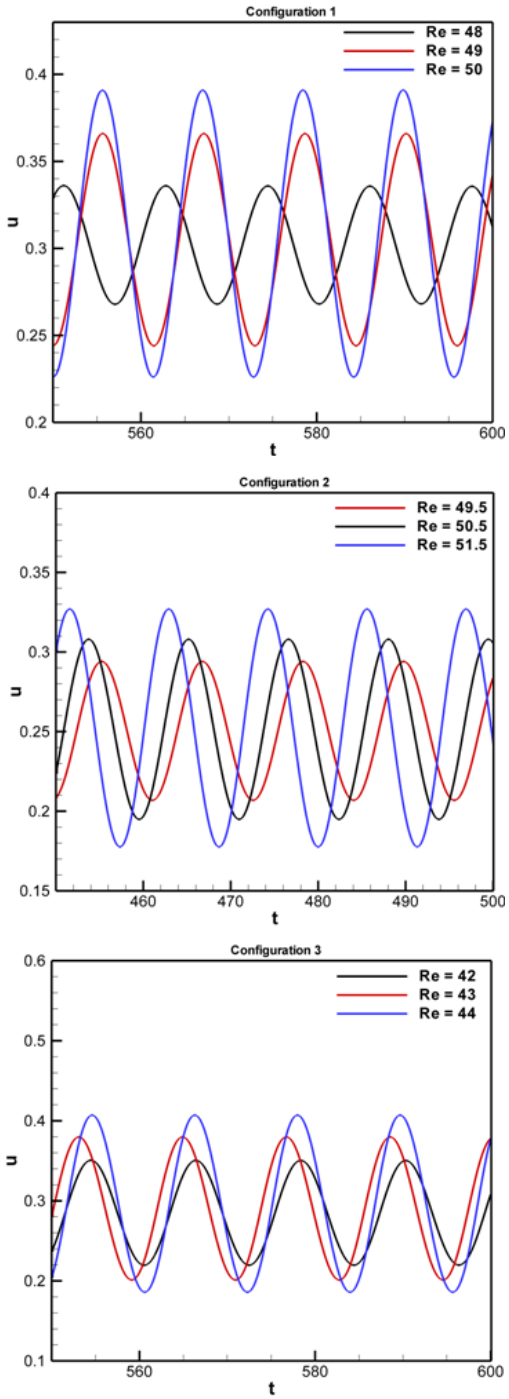

Fig. 4. Temporal variation of the horizontal u-velocity component at location (x=18; y=4.4) relatively to the three considered configurations.

It should be noted that the amplitude of the component of velocity (u or v) is defined as:

$Amp = | u_{i\ max}(A, t) - u_{i\ min}(A, t) | / 2$, where the coordinates of the monitoring point A (18; 4.4) is taken in the wake of the obstacle. During this procedure, we compute the values of the squared amplitudes Amp^2 of velocity components u (A) and v (A).

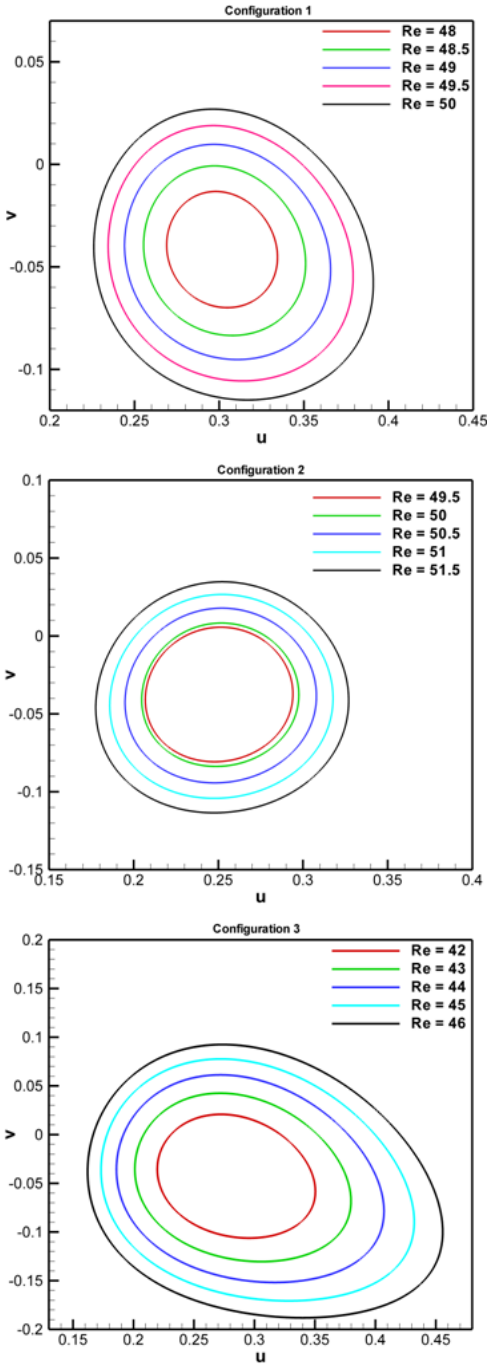

Fig. 5. Phase diagram (v, u) for the three studied configurations at location(x=18; y=4.4).

This allowed us to plot the squared amplitudes of oscillations (Amp^2) versus Reynolds number as depicted in Figure 6.

We find an affine equation such as:

$$Amp^2 = b \times \mathrm{Re} + a$$

Where a and b are coefficients that was determined in each configuration.

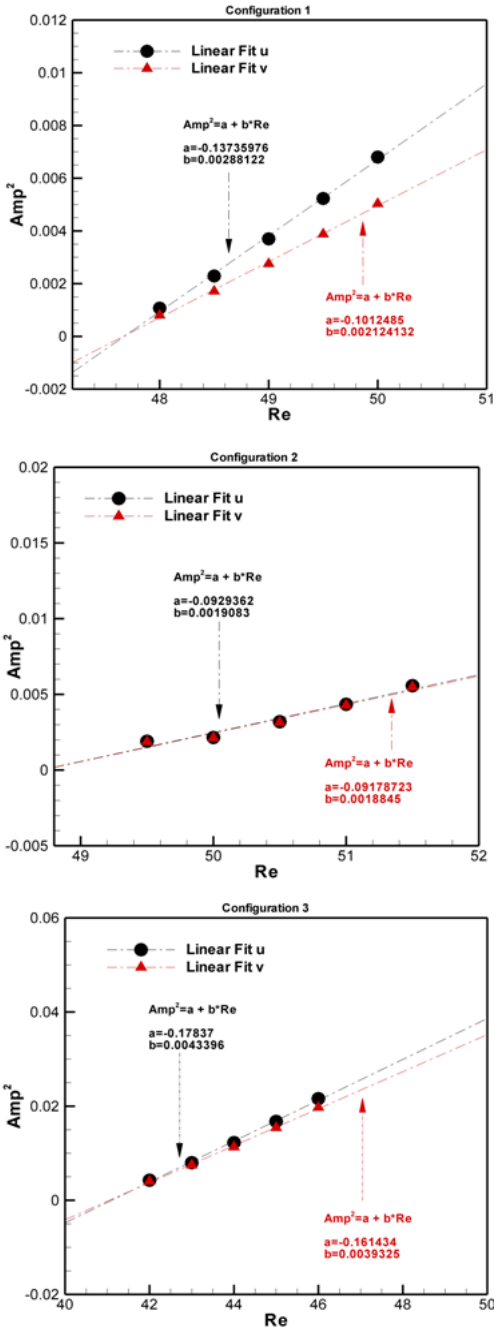

Fig. 6.Variation of the square amplitude of the oscillations of u and v velocity components at the same point as a function of the Reynolds number for the three configurations.

When the amplitude of oscillation is zero (Amp^2 = 0), the value of the critical Reynolds is therefore:

$$\mathrm{Re}c = -(a/b)$$

Extrapolation of each curve to zero amplitude allowed us to determine the value of the critical Reynolds number Rec for which the transition to the periodic regime occurs. The values of both constants a and b were determined (Figure 6) and values of the critical Reynolds number Rec for the different configurations are listed in Table 1.

In order to study the effect of the geometry of the obstacle on the dynamics of the flow structure, we performed a comparison between the three configurations. First, we started by analyzing the releases in the near vortex depending on the Reynolds number wake and wenoted that an unsteady behavior

Table 1 Numerical values of the critical Reynolds number of the first bifurcation for each configuration

configuration	Rec
1(ε=1)	47.7
2(ε=0)	48.7
3(ε=2)	41.0

of the flow appears in the configuration 3 (ε = 2) and in the configuration 1 (ε = 1) and finally in the configuration 2 (ε = 0). We can conclude that the top of the obstacle causes a retardation of the appearance of unsteadiness when ε = 0 and ε = 1 and tends to stabilize the wake. For this reason we find that the transition to the unsteady regime begins firstly in the third configuration, then in the first one and finally occurs at the second configuration. Consequently, this may explain that Rec(ε=0)> Rec(ε=1)> Rec(ε=2).

5. CONCLUSION

A numerical study on the effects of different arrangements of two shapes on two-dimensional flow structure and its stability was investigated. Numerical experiments were performed using a numerical code based on a finite volume formulation, the projection method and a multi-grid-type acceleration. We started our results by validating the code with a problem in the literature and found good agreement between the available results. Thereafter we analyzed the flow structure for different Reynolds numbers and we noticed that for Re <Rec , the flow is stable and steady and symmetrical with respect to the longitudinal axis. Downstream the obstacle, a wake appears formed by two counter rotating eddies attached to obstacle which remains almost symmetrical. For Re> Rec, a change in vortex is seen with a development of the vortex street of Von- Karman with also an increase in the wake zone. Indeed vortex shedding starts in configuration 3 (ε = 2) and configuration 1 (ε = 1) and finally the configuration 2 (ε = 0).On another hand, we found that the flow regime remains oscillatory beyond Rec and a steady flow regime cannot persist beyond this critical value. Moreover, we noticed that the amplitude of the oscillations increases with Re. As a result, the flow after the

critical point is unstable and periodic in time and the bifurcation point of instability is a Hopf bifurcation.

We also found that the Reynolds number for which transition to the unsteady state starts, is smaller for configuration number three, i.e., Rec=41.0 Finally, we can conclude that the top obstacle position plays an important role for the stability of the flow. Indeed, the flow will be more stable for configuration number two.

REFERENCES

Ben Cheikh,N., B. Ben Beya and T.Lili (2007). Benchmark solution for time-dependent natural convection flows with an accelerated full-multigrid method. Numer.*Heat Transfer B* 52, 131-151.

Ben Cheikh,N., B. Ben Beya and T. Lili (2008).A multigrid method for solving the Navier–Stokes/Boussinesq equations.Commun.*Numer.Meth.Engng*. 24, 671-681.

Berrone,S., V. Garbero and M.Marro (2011). Numerical simulation of low-Reynolds number flows past rectangular cylinders based on adaptive finite element and finite volume methods. *Computers & Fluids*40, 92-112.

Bhattacharyya,S. and D. K. Maiti (2004). Shear flow past a square cylinder near a wall. *International Journal of Engineering* Science 42, 2119-2134.

Bhattacharyya, S. and S.Dhinakaran (2008).Vortex shedding in shear flow past tandem square cylinders in the vicinity of a plane wall.*Journal of Fluids and Structures* 24,400-417.

Breuer, M., J. Bernsdorf, T. Zeiser and F. Durst (2000). Accurate computations of the laminar flow past a square cylinder based on two different methods: lattice-Boltzmann and finite-volume. *Int. J. Heat and Fluid Flow* 21, 186-196.

Brown,D. L., R. Cortezand M. L. Minion (2001).Accurate projection methods for the incompressible Navier–Stokes equations.*Comput. Mech*. 168, 464-499.

Chatterjee,D. and B. Mondal (2011).Effect of thermal buoyancy on vortex shedding behind a square cylinder in cross flow at low Reynolds numbers.*Int. J. Heat Mass Transfer* 54, 5262-5274.

Chen,J.-H., W. G. Pritchardand S. J. Tavener (1995).Bifurcation for flow past a cylinder between parallel planes.*J. Fluid Mech*. 284, 23-41.

Dhinakaran, S.(2011). Heat transport from a bluff body near a moving wall at Re= 100. *Int. J. Heat Mass Transfer* 54, 5444-5458.

Franke,R., W. Rodi and B. Schönung (1990). Numerical calculation of laminar vortex-shedding flow past cylinders.*J. Wind Eng. Ind*. Aerodyn. 35, 237-257.

Galletti,B., C. H. Bruneau, L. Zannetti and A. Iollo (2004).Low-order modelling of laminar flow regimes past a confined square cylinder.*J. Fluid. Mech*. 503, 161-170.

Guo, J. and P. Y. Julien (2008).Application of the Modified Log-Wake Law in Open-Channels.*Journal of Applied Fluid Mechanics* 1(2), 17-23.

Hortmann,M., M. Peric and G. Scheuerer (1990). Finite volume multigrid prediction of solutions laminar natural convection: Bench-Mark. *Int. J. Numer. Meth. Fluids* 11, 189-207.

Jackson,C. P. (1987). A finite-element study of the onset of vortex shedding in flow past variously shaped bodies.*J. Fluid Mech*. 182, 23-45.

Kelkar,K. M. and S. V. Patankar (1992).Numerical prediction of vortex shedding behind a square cylinder.*Int. J. Numer. Meth*. Fluids 14, 327-341.

Mukhopadhyay,A., G. Biswas and T.Sundararajan (1992).Numerical investigation of confined wakes behind a square cylinder in a channel.*Int. J. Numer. Meth. Fluids* 14, 1473-1484.

Noack,B. R. and H. Eckelmann (1994).A global stability analysis of the steady and periodic cylinder wake.*J. Fluid Mech*. 270, 297-330.

Qu,L., C.Norberg, L. Davidson and S. H. Peng (2013).Quantitative numerical analysis of flow past a circular cylinder at Reynolds number between 50 and 200.*Journal of Fluids and Structures* 39, 347-370.

Sahin,M. and R. G. Owens (2004).A numerical investigation of wall effects up to high blockage ratios on two-dimensional flow past a confined circular cylinder.*Phys. Fluids* 16, 1305-1320.

Sohankar,A., C. Norberg and L. Davidson (1998). Low Reynolds number flow around a square cylinder at incidence: Study of blockage, onset of vortex shedding and outlet boundary condition. *Int. J. Numer. Meth.Fluids* 26, 39-56.

Straatman,A. G. and R. J. Martinuzzi (2003).An examination of the effect of boundary layer thickness on vortex shedding from a square cylinder near a wall. J. *WindEng. Ind. Aerodyn.* 91, 1023-1037.

Turki,S., H. Abbassi and S. B. Nasrallah (2003).Effect of the blockage ratio on the flow in a channel with a built-in square cylinder.*Comput. Mech*. 33, 22-29.

Wang, Y., Y. Xin, Zh. Gu, Sh. Wang, Y. Deng and X. Yang (2014). Numerical and experimental investigations on the aerodynamic characteristic of three typical passenger vehicles.*Journal of Applied Fluid Mechanics*

7(4), 659-671

Yang, X. and Zebib, A. (1989).Absolute and convective instability of a cylinder wake.*Phys. Fluids* A, 1, 689–696.

Zhou,L., M. Cheng and K. C. Hung (2005).Suppression of fluid force on a square cylinder by flow control.*Journal of Fluids and Structures* 21, 151-167.